

# Intraoperative forces and moments analysis on patient head clamp during awake brain surgery

Danilo De Lorenzo · Elena De Momi ·  
Lorenzo Conti · Emiliano Votta · Marco Riva ·  
Enrica Fava · Lorenzo Bello · Giancarlo Ferrigno

Received: 25 July 2012 / Accepted: 17 November 2012 / Published online: 2 December 2012  
© International Federation for Medical and Biological Engineering 2012

**Abstract** In brain surgery procedures, such as deep brain stimulation, drug-resistant epilepsy and tumour surgery, the patient is intentionally awakened to map functional neural bases via electrophysiological assessment. This assessment can involve patient's body movements; thus, increasing the mechanical load on the head-restraint systems used for keeping the skull still during the surgery. The loads exchanged between the head and the restraining device can potentially result into skin and bone damage. The aim of this work is to assess such loads for laying down the requirements of a surgical robotics system for dynamic head movements compensation by fast moving arms and by an active restraint able to damp such actions. A Mayfield® head clamp was tracked and instrumented with strain gages (SGs). SG locations were chosen according to finite element analyses. During an actual brain surgery, displacements and strains were measured and clustered according to events that generated them. Loads were inferred from strain data. The greatest force components were exerted vertically (median 5.5 N, maximum 151.87 N) with frequencies up to 1.5 Hz. Maximum measured displacement and velocity

were 9 mm and 60 mm/s, with frequencies up to 2.8 Hz. The analysis of loads and displacements allowed to identify the surgery steps causing maximal loads on the head-restraint device.

**Keywords** Awake brain surgery · Force sensors · Intraoperative force/moments measurement · Head clamp · Head rest · Motion compensation

## 1 Introduction

In some brain surgery procedures, such as deep brain stimulation (DBS), drug-resistant epilepsy surgery and brain tumour surgery, the patient is intentionally awakened for performing functional and electrophysiological assessments aimed at mapping the neural bases of motor, sensory and cognitive functions. In DBS, for example, employed in the treatment of Parkinson's disease and other movement disorders, electrophysiological brain activity is recorded to refine the pre-planned magnetic resonance imaging (MRi) localization of the target [5, 8]. In this procedure, the patient must be intraoperatively awakened to check the effect of the electrical stimulation [11] and of other neurophysiologic tests for best DBS electrode placement [14].

Patients are also awakened in neuro-oncological open skull surgeries [21] to appropriately evaluate the somato-sensory and cognitive functions, such as language (e.g., spontaneous speech, object naming, comprehension, etc.), calculation, memory, reading, etc., which are investigated by means of direct cortical and subcortical electrical stimulation and neuro-psychological intraoperative tests [21]. Having this been done, the extent of tumor resection is maximized, while minimizing the risk of irreversible postoperative deficits [6].

---

D. De Lorenzo (✉) · E. De Momi · L. Conti · E. Votta ·  
G. Ferrigno  
Bioengineering Department, Politecnico di Milano,  
Piazza Leonardo da Vinci, 32, 20133 Milan, Italy  
e-mail: danilo.delorenzo@mail.polimi.it

E. De Momi  
Istituto di Tecnologie Industriali ed Automazione,  
Consiglio Nazionale delle Ricerche, Via Bassini 15,  
20133 Milan, Italy

M. Riva · E. Fava · L. Bello  
Neurochirurgia, Istituto Clinico Humanitas, IRCCS,  
Università degli studi di Milano, Via Manzoni 56,  
Rozzano, MI, Italy

In these procedures, as in almost all of brain surgeries, the head is fixed to the surgical table through a stiff-restraint device (e.g., the Mayfield® clamp) to limit undesired movements during surgery. The clamp is fixed to the patient's head by means of surgical pins tapped in the outer part of the skull bones.

Several problems associated with the head clamp fixation have been reported in the literature and that include air embolism, bleeding from the pins and scalp and eye laceration [18]. In addition, intracranial complications were reported in paediatrics neurosurgery [9] and in adult patients [10, 20]. Lee and Lin [10] reported the occurrence of an intracranial epidural hematoma in an adult patient without any prior intracranial pathology after the use of the head clamp during posterior cervical spine surgery. These events are related to loads exchanged by the patient's head and the restraint device, and to the associated displacements. After cortical electrical stimulations, seizures or assessment maneuvers, the head fixation device can undergo displacements due to the loads that are exerted by the patient, the surgeon or accidental events.

This knowledge could be used to define the requirements to optimize restraining devices and designing specific active devices able to damp the patient head movements, and to design the control system of two lightweight robots which will compensate the patient head movements during the operation, as it is planned for the FP7 ICT 270460 ACTIVE project [7]. A parallel kinematics robot, whose end-effector will be attached to the Mayfield® skull clamp, was designed [13] and is about to be developed. To this aim, we equipped an Mayfield® clamp with an on-purpose designed force/moment sensor based on the strain gauges to collect the requirements and specifications for the parallel robot design and for the real-time control loop (maximum allowed head displacements, maximum force/moments exerted by the patient head during a prototypical operation, maximum frequency content of the patient head displacements). In [4] and in [24], SGs were used on restraint devices to measure forces. Among the possible technologies for six axes force-moment sensors design (e.g., piezoresistive, piezoelectric, capacitive etc. [3, 12, 22]), SGs allow for easy customization, guarantee wide design possibilities and are cost-effective.

The sensor was designed to allow the measurement of force/moments values of the patient head. Several works reported the range of force and moments that can be generated by voluntary movements of the neck and of the head. In Vasavada et al. [23], moments during maximum voluntary contractions of neck muscles were measured on 11 men and resulted  $52 \pm 11$  N m during extension and  $30 \pm 5$  N m during flexion. Similar moment values resulted in Seng et al. [19] (52.04 and 31.19 N m during

extension and flexion, respectively). In [15], the isokinetic neck strength profile of a specific population (24-year-old senior elite rugby players) was assessed. The mean flexion moment was 44.04 N m and the mean extension moment was 65.60 N m. However, all these data do not refer to scenarios comparable to neurosurgery procedures in terms of patient body posture and constraints. Indeed, these greatly affect forces and moments exerted by neck muscles. Resazoltani et al. [17] showed that the isometric force and isometric moment of neck extensor muscles are strictly dependent on the location of the thoracic support, i.e., where the torso is restrained. Reported results, measured on a population of 20 healthy women, showed that the maximum isometric force ( $\sim 150$  N) and maximum isometric moment ( $\sim 70$  N m) generated by the neck extensor muscles vary with the length of the lever arm, represented by the different levels of thoracic support.

## 2 Materials and methods

This section describes the experimental set-up and the processing techniques for the quantification of the loads exerted by the patient's head on a specific restraint device during brain surgery, and the corresponding head displacements. The experimental set-up consisted of a system of strain-gage (SG) load sensors and an optical tracking system.

Hence, after describing the restraint device, we present the theoretical background for SG force sensors, the design of the SGs system through finite element (FE) simulations, and the direct experimental measurement of strains on the restraint device, along with the optical tracking system for displacement measurements. Then, the calibration procedure for the experimental measurement system is described. Finally, we provide the details of the signal processing techniques adopted for the quantitative description of loads and displacements in terms of magnitude and frequency content.

### 2.1 The instrumented restraint device

The Mayfield® Ultra 360™ Patient Positioning System, Integralife, (MPPS, Fig. 1b) is a passive 7 degrees of freedom mechanical repositionable device that allows for positioning and fixing the head of the patient during surgical procedures. Once the head is positioned in the desired configuration, the joints of the MPPS are locked to form a rigid structure. In order to measure forces ( $F_x$ ,  $F_y$ ,  $F_z$ ) and moments ( $M_x$ ,  $M_y$ ,  $M_z$ ) acting on its terminal screw, the MPPS was instrumented with seven SGs and an appropriate calibration procedure was performed.

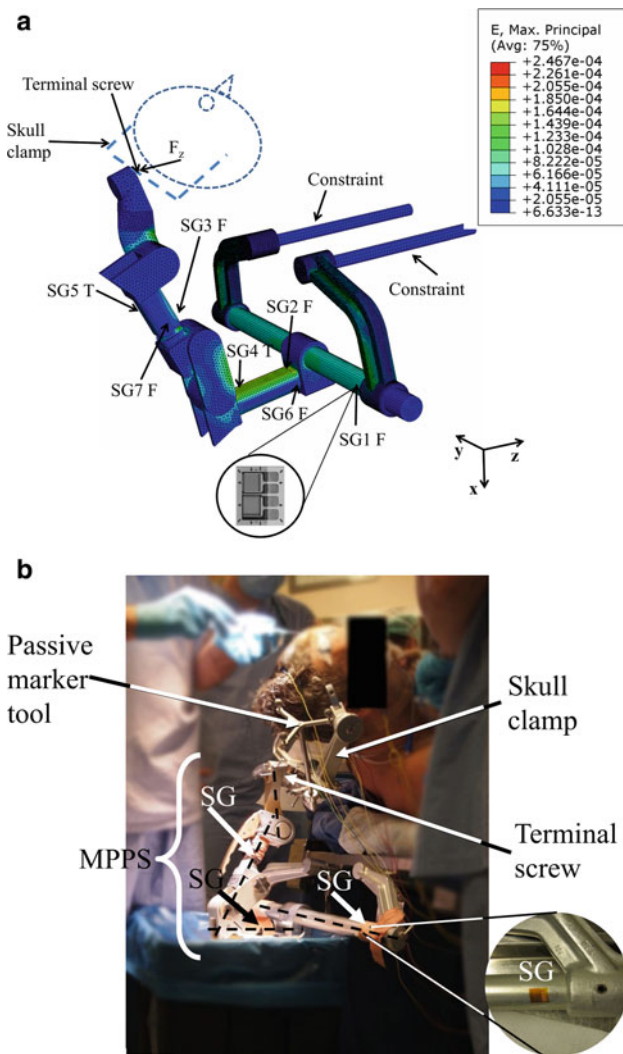


**Fig. 1** **a** CAD model of the Mayfield® patient positioning system (MPPS), constraints, point of application of forces and moments (terminal screw) and SG positions are indicated.  $F$  indicates 90° tee SG rosettes for flexion measurements, while  $T$  indicates 90° tee SG rosettes for torque measurements. The color map shows max principal strains in case of a force applied along the  $z$  axis ( $F_z$ ). **b** Operating room setup. SG locations on the MPPS are shown. The passive marker tool for tracking the MPPS position is also shown, together with the terminal screw (which is coincident with the origin of the reference frame of forces and moments) and the skull clamp attached to it. Dotted lines show the main links of the MPPS

2.2 Loads measurement through SGs: theoretical background

The unknown forces and moments vector  $\mathbf{w} = (F_x, F_y, F_z, M_x, M_y, M_z)$  acts on the terminal screw, where the Mayfield® skull clamp is attached to the MPPS (Fig. 1b). The vector  $\mathbf{s} = (s_1, \dots, s_N)$ ,  $N \geq 6$ , contains the set of the associated SGs output signals (*strains*). Under the hypothesis of infinitesimal strains and linear elastic behavior of the MPPS, the following linear relationship can be written [12]:

$$\begin{bmatrix} s_1 \\ \vdots \\ s_N \end{bmatrix} = \begin{bmatrix} c_{11} & \cdots & c_{16} \\ \vdots & \ddots & \vdots \\ c_{N1} & \cdots & c_{N6} \end{bmatrix} \cdot \begin{bmatrix} F_x \\ F_y \\ F_z \\ M_x \\ M_y \\ M_z \end{bmatrix} = \mathbf{C} \cdot \mathbf{w} \tag{1}$$

The estimation of  $\mathbf{w}$  from  $\mathbf{s}$  and through  $\mathbf{C}$  is accurate if the linear system is well-conditioned, i.e., if the condition number  $C_0$  [12] of  $\mathbf{C}$  is close to 1 (ideally  $C_0 = 1$ ). Differently, small errors in the measured output signals  $\mathbf{s}$  can lead to relevant errors in the computation of  $\mathbf{w}$ . If  $\mathbf{C}$  and the strain signals  $\mathbf{s}$  were known, the force vector  $\mathbf{w}$  could be computed as:

$$\mathbf{w} = \mathbf{Y} \cdot \mathbf{s} \tag{2}$$

where  $\mathbf{Y}$  is the *calibration matrix* [12] defined as the pseudo-inverse of  $\mathbf{C}$ :

$$\mathbf{Y} = (\mathbf{C}^T \mathbf{C})^{-1} \mathbf{C}^T \tag{3}$$

However, in our case,  $\mathbf{C}$  is not known a priori and needs to be determined through calibration, i.e., by applying a set of known load vectors ( $\hat{\mathbf{w}}_1, \hat{\mathbf{w}}_2, \dots, \hat{\mathbf{w}}_k$ ) to the MPPS terminal screw, by recording the corresponding output signal vectors ( $\hat{\mathbf{s}}_1, \hat{\mathbf{s}}_2, \dots, \hat{\mathbf{s}}_k$ ), and by computing  $\mathbf{C}$ , after having solved the systems of linear equations:

$$\mathbf{S} = \mathbf{C} \cdot \mathbf{W} \tag{4}$$

where  $\mathbf{S}$  is the  $N \times k$  strain signal matrix corresponding to the  $k$  applied loads ( $\hat{\mathbf{w}}_1, \hat{\mathbf{w}}_2, \dots, \hat{\mathbf{w}}_k$ ) and  $\mathbf{W}$  is the  $6 \times k$  matrix of loads.

The full form of Eq. (4) is

$$\begin{bmatrix} \hat{s}_{11} & \cdots & \hat{s}_{1k} \\ \vdots & \ddots & \vdots \\ \hat{s}_{N1} & \cdots & \hat{s}_{Nk} \end{bmatrix} = \begin{bmatrix} c_{11} & \cdots & c_{16} \\ \vdots & \ddots & \vdots \\ c_{N1} & \cdots & c_{N6} \end{bmatrix} \cdot \begin{bmatrix} \hat{w}_{11} & \cdots & \hat{w}_{1k} \\ \vdots & \ddots & \vdots \\ \hat{w}_{61} & \cdots & \hat{w}_{6k} \end{bmatrix} \tag{5}$$

Because the system is over-determined,  $\mathbf{C}$  has to be obtained in a least-squares sense, i.e.:

$$\mathbf{C} = \mathbf{S}(\mathbf{W}^T \mathbf{W})^{-1} \mathbf{W}^T \tag{6}$$

2.3 SGs design through FE simulations

A CAD model of the MPPS (Fig. 1a) was implemented using Solidworks® Premium 2009 (Dassault Systèmes, Vélizy, France), and then discretized into 21,000 hexahedral and 683,000 tetrahedral linear elements (approximate average size = 2.5 mm). A sensitivity analysis showed this value to be a very good a trade-off between computational time and accuracy of numerical results, having the elements size increased the computational cost from 5 min to several hours and introducing a difference in the strains computed in the locations of interest by less than 0.5  $\mu$ strain (i.e.,

nearly two orders of magnitude lower than the smallest detected strains). The MPPS was described as made of aluminum alloy (elastic modulus, Poisson ratio, yielding stress and strain equal to 72 GPa, 0.34, 520 MPa and 0.72 %, respectively), which was modeled as a linear elastic material based on the assumption that computed strains would have been lower than the yield limit. To identify the best configuration and location on the MPPS for the SGs, a series of simulations were run through the commercial solver ABAQUS/Standard<sup>®</sup> 6.9 (Dassault Systèmes, Vélizy, France); linearly increasing forces (up to 150 N, 50 N step) and moments (up to 70 N m, 10 N m step) [15] acting along  $x$ ,  $y$  and  $z$  axis were applied to the terminal screw of the virtual model, while constraining the two cylindrical segments shown in Fig. 1a with respect to translations and rotations, so to mimic the real constraint to the surgical bed.

Pairs of adjacent mesh elements were chosen as SG positions on the fixation device (shown in Fig. 1a) where the differences between strains along two perpendicular directions were greater than  $10\mu\epsilon$  (ten times the expected system resolution). The choice of SG positions was also influenced by the need to avoid operative obstruction to the medical staff and to allow relative rotations around the joints of the MPPS during patient head positioning.

A frequency analysis was also performed in the same simulation environment to determine the modes of vibration of the device.

## 2.4 Experimental setup

MPPS strains and head displacements were acquired during a 6-h neurosurgical procedure for removing a left fronto-insular oligo-astrocytoma (World Health Organization Grade II) affecting a 41-year-old patient weighing 84 kg. The procedure was performed at the Neurosurgery Department of the Istituto Clinico Humanitas (Rozzano, Milan, Italy). The scientific and ethical review boards approved the experimental setup and technical specifications of the instrumentation and a proper informed consent was obtained by the patient.

The MPPS was instrumented using 7 strain-gauges the day before the intervention, following indications from FE analysis (Fig. 1a). Flexion and torque ( $F$  and  $T$ , Fig. 1a) 90° tee rosettes SGs (Vishay<sup>®</sup> Precision Group, Malvern, PA, USA) were used ( $350\ \Omega \pm 0.4\%$ ,  $3.3 \times 2.0$  mm area). The SGs were connected in a half bridge configuration using remote sense wires to eliminate gain errors due to the resistance of the excitation leads.

Signals were acquired using a NI Compact DAQ and a NI 9237 Bridge Module (National Instruments<sup>®</sup> Austin, TX, US), with 1,613 Hz sampling frequency. The bridge module

was connected to a notebook PC via USB interface. Data collection was performed using Labview<sup>®</sup> 2011 (National Instruments<sup>®</sup>, Austin, TX, US). The final experimental setup in the operating room is shown in Fig. 1b.

Head displacements were measured using the optical tracking system Polaris Vicra<sup>®</sup> (Northern Digital Inc., Ontario, Canada) (stated accuracy 0.25 mm, acquisition frequency 20 Hz). The optical localizer acquired the position of a passive marker tool attached to the skull clamp. Displacement signals were acquired using NDI Tool Tracker SW (Northern Digital Inc., ON, Canada).

Events occurred during the intervention were recorded on paper and classified according to four different typologies:

1. *Surgeon action* events caused by the action of the surgeon or by the medical staff (e.g., use of surgical driller, suturing, scalp clips application, use of aspirator...).
2. *Induced patient movement* patient movements caused by direct cortical and subcortical electrical stimulation or requested by the medical staff (e.g., use of stimulator on cortical areas, patient asked to speak or count or to open and close his hand...).
3. *Patient movement* voluntary and physiological (e.g., breathing) patient movement not requested or elicited by the medical staff (e.g., muscles activity, unrequested head, leg and foot movement, breathing chest movement...).
4. *Accidental movements* patient movement not fitting inside the above categories (e. g. right leg slightly falling out of bed...).

## 2.5 Calibration

To successively derive forces/moments from measured MPPS strains, after the intervention, when the patient head and the skull clamp had already been detached from the clamp, a calibration was performed on the SGs system without changing the MPPS configuration. An orthonormal reference frame was defined (Fig. 2a) as follows: the origin was coincident with the terminal screw, the  $x$  axis was the gravity force direction and the  $z$  axis was perpendicular to  $x$  and laying in the sagittal plane. Forces and moments were applied using a system of weights and pulleys (Fig. 2a, b).  $F_x$  was applied by directly connecting weights to the terminal screw, while forces along  $z$  and  $y$  directions ( $F_y$  and  $F_z$ ) were applied through a pulley, as shown in Fig. 2b. The perpendicularity between  $F_z$  and  $F_x$  and between  $F_y$  and  $F_x$  was obtained using bubble levels. Moments were applied using an arm attached to the terminal screw off the MPPS (Fig. 2a).

Based on the assumption of linear mechanical response of the MPPS, the applied loads ranged between 5 and 55 N for force components and between 0.8 and 5.5 N m for moments.

The **C** matrix coefficients ( $c_{ij}$ ) were computed solving the systems of linear equations (Eq. 4), as previously described.

### 2.6 Signal processing

The acquired force/moment and displacement signals were processed using MATLAB® 2011a (Mathworks®, Natick, MA, USA).

The SGs electronic signal bias was recorded for 5 min and subtracted from all the acquired strain signals. To reduce the computational load, strain signals were decimated to 201.6 Hz sampling rate. To avoid aliasing, data were filtered with a 121th order low pass equiripple FIR

filter (50 Hz cut-off frequency, 100 Hz stop-band frequency, 0.001 dB pass-band ripple and 50 dB stop-band attenuation) before re-sampling. The values of forces and moments (**w**) were estimated multiplying the half bridge outputs, **s**, times the calibration matrix **Y**, as described in Eq. (1).

For each type of event  $q = 1 \dots 4$ , the force/moment difference ( $\Delta w_{ij}^q$ ) between the actual force/moment value and the event average force/moment value was computed for each temporal instant  $k$ , such as:

$$\Delta w_j^q(k) = w_j^q(k) - \left[ \frac{1}{N} \sum_{k=1}^N w_j^q(k) \right] \tag{7}$$

where  $j = 1, \dots, 6$  and  $N$  is the number of time samples in the considered  $q$ th event.

The values of stationary baseline forces and moments due to the patient head, shoulders and skull clamp loads were estimated as the average on the last 10 s of the intervention, with the patient asleep (without any movements or applied load).

Head velocity and acceleration were computed from displacement data. The velocity vector was computed by a central finite difference scheme:

$$v(k) = \frac{\mathbf{p}(k+1) - \mathbf{p}(k-1)}{2t_s} \tag{8}$$

where  $k$  denotes the sample number,  $\mathbf{p} = [x, y, z]^T$  and  $t_s$  the sampling period ( $t_s = 50$  ms).

Acceleration was computed by Eq. (9):

$$a(k) = \frac{\mathbf{v}(k+1) - \mathbf{v}(k-1)}{2t_s} \tag{9}$$

Of note, during induced patient movement events head displacements could not be measured because medical staff was hiding the line of sight of the optical tracking device.

### 2.7 Evaluation metrics

To evaluate the resolution of the force/moment sensor, we computed the root mean square (RMS) residual calibration error  $e$  between known applied force/moment vectors **w** and the force/moment estimations  $\hat{w}$ , computed using the strain signals as:

$$e_j = \sqrt{\frac{1}{M} \sum_{k=1}^M (w_{jk} - \hat{w}_{jk})^2} \tag{10}$$

where subscript  $j = 1, \dots, 6$  are the six **w** components (force and moment) and  $M$  is the number of calibration acquisitions.

Force/moments, displacements, velocities and accelerations signals of each event class were evaluated using

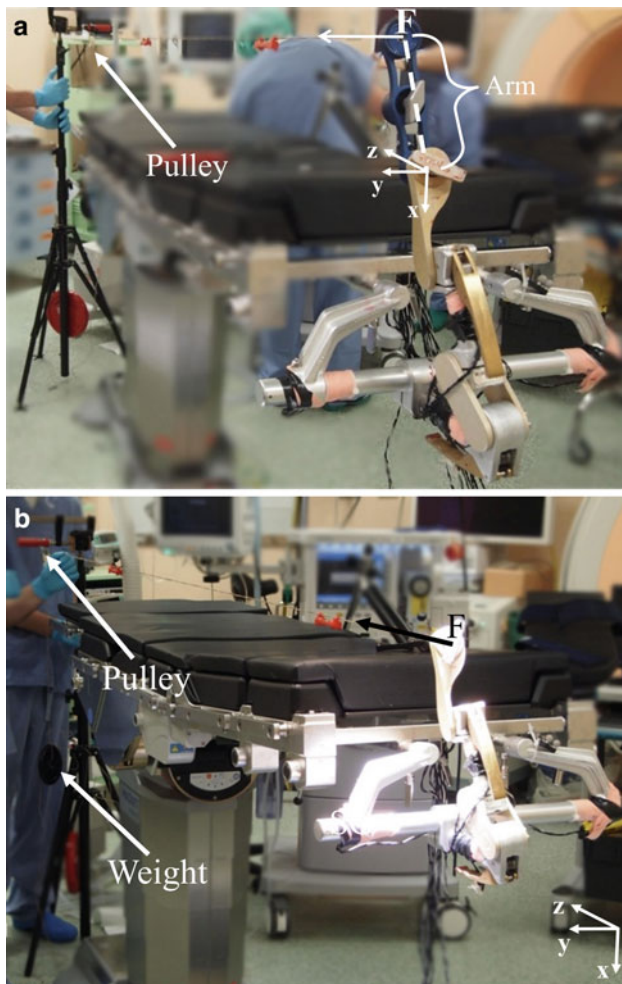
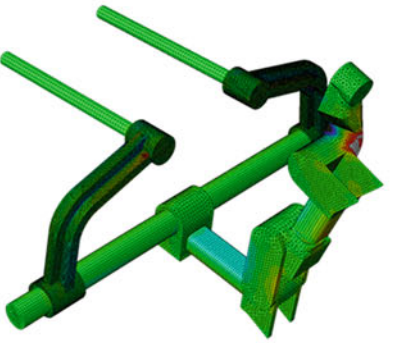
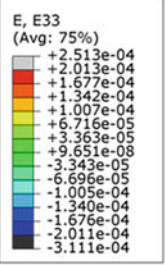
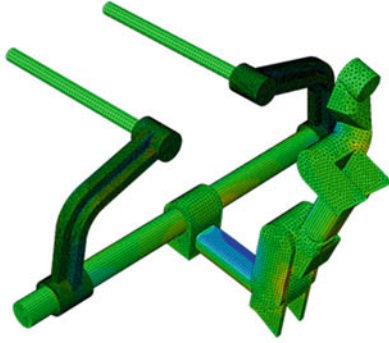
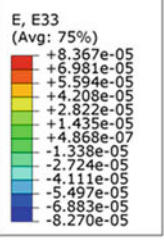
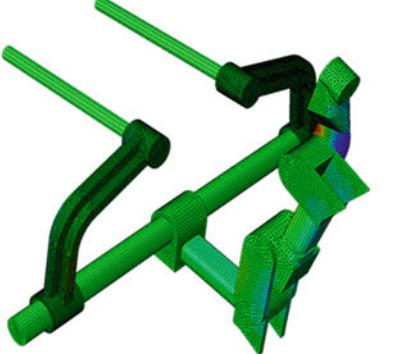
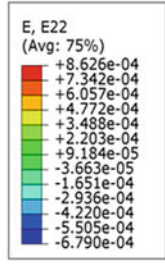
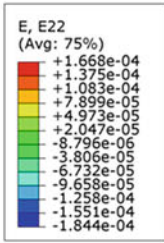
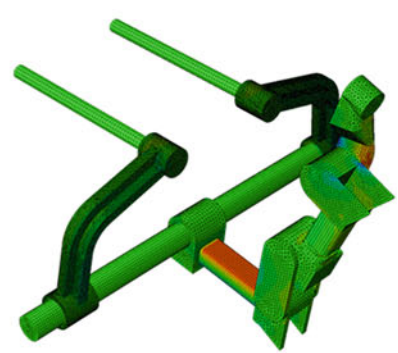
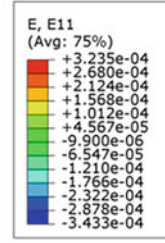
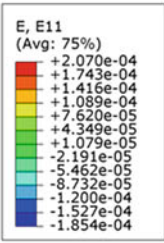


**Fig. 2** **a** Sensor calibration: application of a moment ( $M_y$ ). The force  $F$  is applied along the  $z$  axis direction using a pulley. **b** Application of  $F$  along the  $z$  axis. The reference frame is shown

**a**



**b**

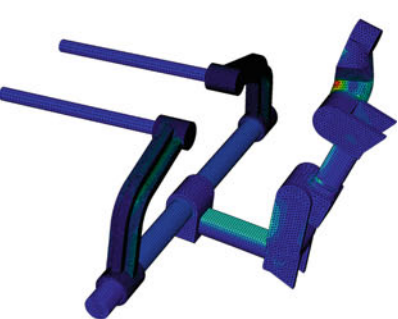
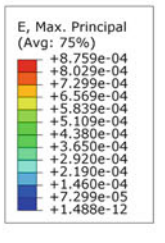
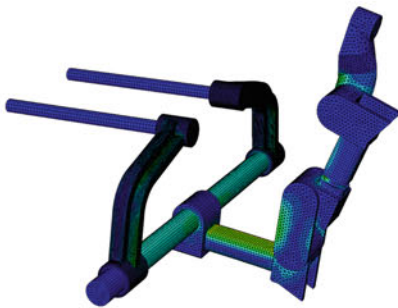
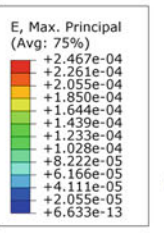


**Fig. 3 a** Color maps of the strains along the three direction:  $E_{xx} = E_{22}$ ,  $E_{yy} = E_{33}$ ,  $E_{zz} = E_{11}$ . The three panels in the left column correspond to a 150 N applied force  $F_z$ . In the right column a 70 N m  $M_y$  moment was applied. From top to bottom  $E_{zz}$ ,  $E_{xx}$  and  $E_{yy}$  are shown. **b** Principal strain color maps for a maximum 150 N applied force (on the left) and for a maximum applied 70 N m moment (on the right)

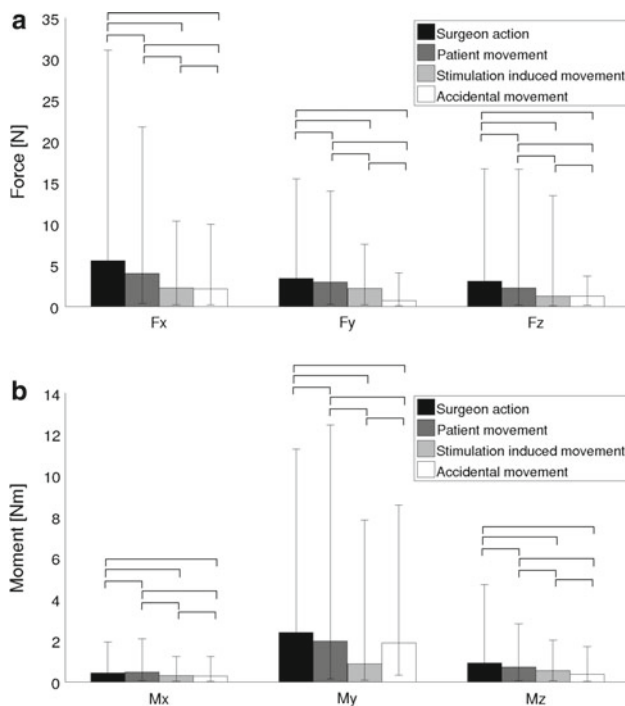


**Fig. 4** Forces (a) and moments (b) during the whole intervention for each event class. Median values, 5th and 95th percentiles are reported. Statistically significant differences are reported with brackets ( $p < 0.05$ )

Lilliefors test to test if data were normally distributed ( $\alpha = 0.05$ ). Kruskal–Wallis test ( $\alpha = 0.05$ ), with Dunn–Sidák post hoc, was performed to compare force and moment differences ( $\Delta w_j$ ), displacement, velocity and

acceleration measurements among different classes of events.

Frequency content of loads, displacements and velocities for each class of event was computed using the power spectrum density (PSD) with the modified covariance method [2]. To identify the frequency content, we used the method described in [2]. A practical upper bound is represented by the frequency at which the signal to noise ratio (SNR) falls below a predefined threshold (Th). The threshold is computed as:

$$Th = k \cdot N \tag{11}$$

with

$$N = \frac{1}{10} \int_{30\text{Hz}}^{50\text{Hz}} PSD(f)df \tag{12}$$

and  $k = 50$ , as described in [2]. We chose the frequency interval 30–50 Hz for noise evaluation (Eq. 12), where the PSD function is flat, reasonably no frequency content due to motion is noticeable, and the Nyquist frequency (100.8 Hz) is twice as high as the highest considered value.

### 3 Results

Figure 3a, b shows the strain map for the maximum applied force and for the maximum applied moment on the MPPS model, respectively. The strain color maps for each applied load (an example is reported in Fig. 3a) were used to chose SG positions. Maximum values of simulated strains (Fig. 3b) were  $2.62 \times 10^{-4}$  for the applied force and  $1 \times 10^{-3}$  for the moment, below the yield strain value (0.71 %).

The maximum strain value corresponding to the SG signals acquired during the experiments was 0.33 %; thus, confirming the hypothesis of small strains and of linear behavior of the system.

**Table 1** RMS errors for each force component after experimental calibration; head, shoulders and skull clamp force and moment static values; absolute maximum values during the entire intervention, for each force and moment components

	$F_x$ (N)	$F_y$ (N)	$F_z$ (N)	$M_x$ (N m)	$M_y$ (N m)	$M_z$ (N m)
RMS calibration errors	2.74	2.09	2.74	0.12	0.96	0.65
Head, shoulder and skull clamp static load	132.65	−15.01	−69.24	−5.67	65.3	10
Max magnitude	151.87	94.71	71.87	34.60	68.69	60.49

**Fig. 5** Forces and moments acting on the MPPS during the skull opening phase. Force/moment perturbation due to the surgical driller action is clearly visible in the [0–10 s] time window

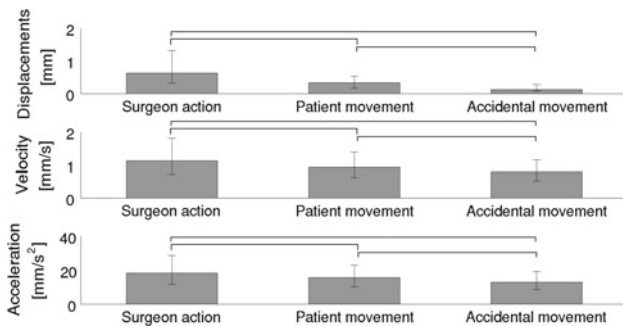
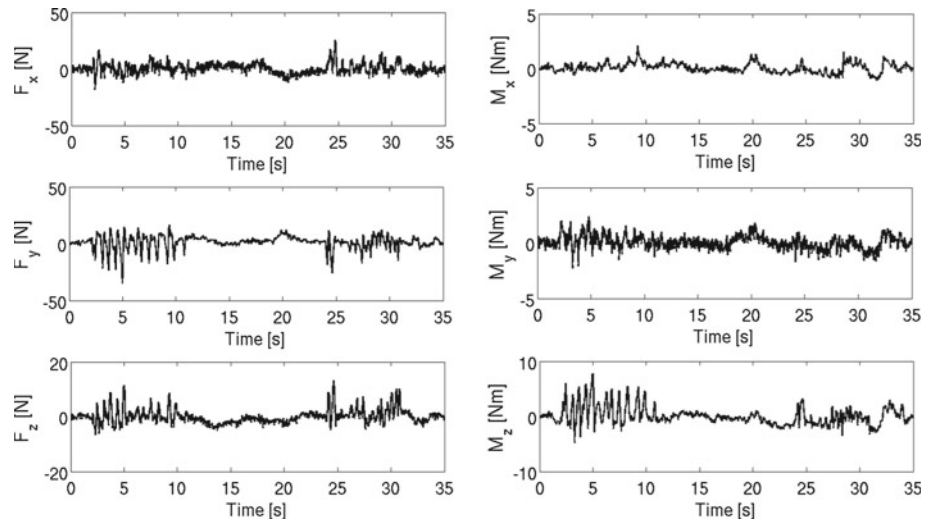


**Fig. 6** Displacements, velocities and accelerations during the whole intervention for three of the four types of events. Median values, 25th and 75th percentiles are reported. Statistically significant differences are reported with brackets ( $p < 0.05$ )

3.1 Load measurements analysis

The force sensor matrix **C**, obtained with the experimental calibration, resulted:

$$C = 10^{-6} \times \begin{bmatrix} -0.0755 & 0.0677 & 0.5440 & 0.3297 & 0.8652 & -0.5435 \\ 0.0546 & 0.0511 & 0.1676 & -0.0139 & 0.7694 & -0.6015 \\ 0.1683 & -0.1838 & 1.3791 & -0.3725 & 3.5515 & -0.2659 \\ -0.1382 & 0.089 & -0.2736 & 0.4664 & -1.4022 & -0.5667 \\ 0.2031 & 1.2366 & -0.0161 & 0.3309 & -0.0942 & -4.2121 \\ 0.0047 & -0.1596 & 0.0669 & 2.3994 & -0.0956 & -1.0662 \\ -0.0269 & 0.2155 & -0.333 & -3.3425 & -0.7471 & 0.0554 \end{bmatrix}$$

The condition number ( $C_0$ ) is 69.92.

Calibration RMS errors are always less than 3 N for forces and 1 N m for moments. Magnitude of forces and moments (median, 5th and 95th percentile) are reported in Fig. 4. Highest values correspond to surgeon actions (median value 5.5 N for force along the vertical direction and 2.4 N m for  $M_y$ ), while smallest values correspond to accidental movements (median value 0.68 N for  $F_y$  and 0.28 N m for  $M_z$ ). Maximum values of the six components of vector **w** during the whole intervention duration and the

values of steady forces and moments due to the patient head, shoulders and skull clamp loads are reported in Table 1. Maximum force component ( $F_x$ ) is along the vertical direction (151.87 N), while maximum moment is directed along the y axis ( $M_y = 68.9$  N m). Maximum contribution of steady loads is along  $F_x$  (132.65 N) and  $M_y$  (65.3 N m).

An example of a surgeon action signal (phase of skull opening, using the surgical driller) is reported in Fig. 5.

Displacement values are in the range of a millimeter (median value) during surgeon actions, and maximum value reached 9 mm during the drilling phase (Fig. 6). During patient movements and accidental movements, displacements were always below 0.35 mm as median value. Velocities median values are close to 1 mm/s for all the event types with a maximum value of 60 mm/s during surgeon actions. Median accelerations are about 20 mm/s<sup>2</sup> in all the four types of events frequency content

The first natural frequency of the device computed in the simulation was 62.67 Hz. Frequency content of the force and moment signals is in the range 0–2.8 Hz. Larger frequency contents are reported for  $F_y$  (median value 0.69 Hz) and for  $M_x$  (median value 1.12 Hz) during surgeon action and accidental movements, respectively (Fig. 7). Lower frequency content correspond to stimulation induced (using stimulation frequency range 0.5–2 Hz) movements (median value 0.1 and 0.47 Hz for  $F_x$  and  $M_y$ , respectively). Nevertheless, the differences are statistically significant exclusively between surgeon actions and patient movements along vertical direction ( $F_x$ ).

The overall displacement frequency bandwidth is between 0.13 and 1.39 Hz as a median value (Fig. 8). Larger frequency content is due to surgeon actions (up to 1.39 Hz). The lower frequency content corresponds to accidental movements (0.13 Hz, median value).

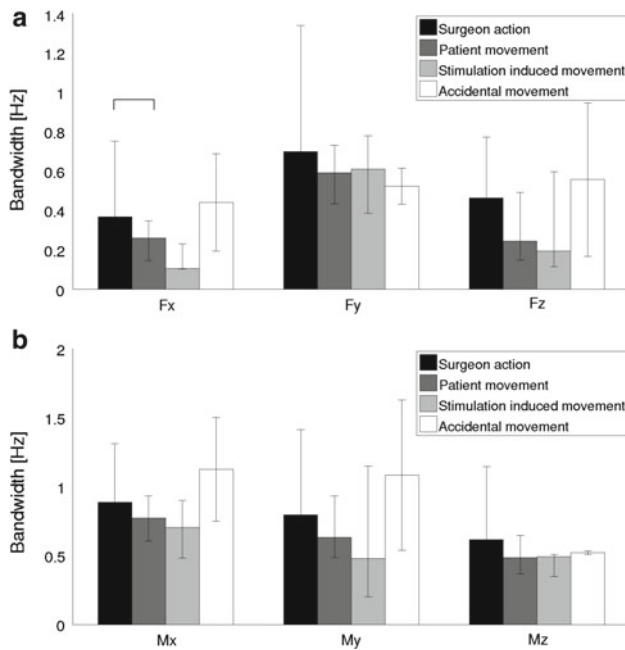


**Fig. 7** Force (a) and moment (b) frequency content during the whole intervention for each type of event. Median values, 25th and 75th percentiles are reported. Statistically significant difference is reported with a *bracket* ( $p = 0.036$ )

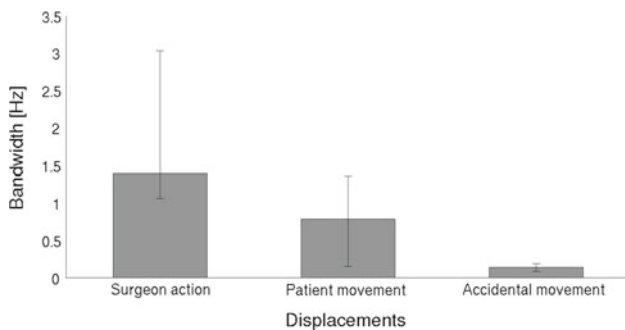


**Fig. 8** Displacements' frequency content during the whole intervention for three of the four types of events. Median values, 25th and 75th percentiles are reported. No statistical difference among all the histograms ( $p = 0.053$ ) was found

Characteristic signal patterns were observed in several segments of the whole intervention at 0.2, 0.5 and 0.7 Hz. In particular, a 0.2 Hz pseudo-sinusoidal signal pattern, related to the patient breathing, was acquired during the early initial phase of the intervention when the patient was asleep and the surgery had not started yet (force range:  $\pm 2$  N).

Signal patterns at 0.5 and 0.7 Hz are related to stimulation for motor-evoked potentials (MEP) recordings with force amplitude up to  $\pm 5$  N.

#### 4 Discussion

Intraoperative measurements were carried out at Istituto Clinico Humanitas, IRCCS (Milano, Italy) to obtain quantitative information about forces and moments exerted by the patient's head during awake neurosurgical interventions. Intraoperative force measurements could directly monitor forces exchanged between the patient skull and the pins. The aim of the data analysis was to estimate the requirements for an active head fixation device to be used in awake neurosurgical procedures, able to damp the possibly occurring head movements [13] and for a two-arm robotic surgical system able to compensate such movements [7]. Awake surgery with cortical stimulation was chosen as a paradigmatic scenario because we expected the highest stresses on the head frame and maximum displacements. Data were acquired during a single surgical intervention, since the operating room availability was limited and due to the strict patient's inclusion criteria. Nevertheless, we believe that the amount of data acquired is exemplary of a variety of possible events in the operating room during an awake neurosurgical intervention. In addition, when considering that maximum magnitude of forces and moments corresponded to surgeon actions, the results of this study are likely valid also for asleep surgery. Further intraoperative acquisition trials will allow comparing our findings even in asleep surgery and with different configurations and types of head rests.

A system of seven double SGs was designed, to measure the strains of the MPPS links during the intervention. During patient preparation, the surgeon sets the MPPS configuration and the patient head pose with respect to the MPPS. In our work, we considered the Mayfield® skull clamp and the patient head as a single body exerting loads on the MPPS.

The design and implementation of force/moment sensors to be used during surgical interventions had to fulfill the operating workspace constraints, electrical safety, sterilization and biocompatibility [16, 22] issues. Forces and moments were estimated after a calibration procedure. The force sensor was calibrated after the surgery, to maintain the MPPS configuration used during the intervention, and thus having consistency between the calibration and measurement set-ups.

The optimization of force sensitivities was challenging due to the imposed MPPS structure. Generally, in force sensor design, the structure is designed on purpose to maximize the sensitivity isotropy [1]. In our case, the structure was designed by the manufacturer of the MPPS and SG location was determined on a reverse engineered CAD model of the MPPS by FE simulations analysis. The MPPS was considered as a whole rigid body; simulations

did not consider joints clearance and the corresponding friction phenomena. Furthermore, the choice of SG positions was influenced by the need to not modify how the medical staff fixed the MPPS on the patient head and to not limit the possible relative movements of the MPPS arms. When considering the geometry of the MPPS device, a completely uncoupled system is not obtainable, and therefore cross-sensitivities exist. A particular strain signal corresponding to a force component is affected by the application of any of the other force components.

Calibration force and moments were well above the median force/torque values. Loads applied during the calibration procedure led to linear strains measurements.

The condition number ( $C_0$ ) of the experimental calibration matrix (69.92), suggests that the force/moment sensitivities among all the six axes are not equal. This is confirmed also by the different values of the calibration residuals among the forces and the moments. However, residual calibration errors values (max RMSE value 2.74 N and 0.96 N m for forces and moments, respectively) and static force/moments noise standard deviation (1.93 N and 0.43 N m for forces and moments, respectively) are more than one order of magnitude lower than maximum load values found during the intervention, for all components.

SG number 7 (Fig. 1a) showed a positive drift during the first 2 h of the intervention, caused by temperature variation, which was compensated.

Events were classified into four typologies to compare the surgical workflow steps. Maximum values of forces and moments were measured when the surgeon used the surgical driller and the dissector in order to open the skull and in the last phase of the intervention, during suturing. In these phases, the medical staff directly applies forces on the head of the patient. Maximum registered force was 151.87 N along  $x$  direction (perpendicular to the floor), this is plausible considering the patient's head position with respect to the defined reference frame. Load values due to patient movements are higher than those due to stimulation and are generally less than surgeon actions, except for moments around  $x$  and  $y$  axis. It is worth considering that the medical staff never asks to the patient to move the head and stimulation induced movements are always arm or leg movements that do not involve direct application of loads on the MPPS. Moreover, patient unexpected movements are often considered as reactions due to pain or uncomfortable position of the body that indirectly involve application of loads on the skull clamp.

For all the types of events, the frequency content is below 1.12 Hz as median value, with a maximum value of 2.8 Hz. As said, the surgeon usually performs slow movements and the patient is sedated. Peaks around 0.5–0.7 Hz and 0.2 Hz are mainly caused by motor-evoked potentials and patient breathing, respectively. Improvements

in data interpretation could be expected by integrating the evaluation of the load signals with the analysis of vital parameters monitoring signals (ECG, EEG or blood pressure), EMG or electrical stimulation signals (e.g., MEP).

The natural frequency of the device, computed in the simulation environment, is 62.67 Hz, which is more than one order of magnitude greater than the maximum frequency content obtained from the experimental data and guarantees that the results are not affected by the device dynamics.

The head displacements during the whole intervention were measured using an optical localization system. The maximum values of displacement, velocities and accelerations were found in case of surgeon actions (9 mm for displacements, 0.06 m/s for velocity and 0.8 m/s<sup>2</sup> for acceleration) with frequency content up to 1.39 Hz as median value, which is comparable with the frequency content of the load signals.

This work is the first study investigating intraoperative head loads on the MPPS during awake brain surgery, and it thus represents a starting reference in the field. In addition, the possibility to measure forces and moments exerted by the patient's head during neurosurgical awake procedures on the head fixation device is a starting point for the analysis of the head clamp side effects and toward their reduction.

Such measurement are important since their collection can improve the devices used in the operating room to reduce discomfort to the patient when he or she is awakened for functional testing and/or to avoid harm to the skull due to high pin pressures. Active devices for head holding can be designed to have a controllable stiffness of the head clamp during the phases of the surgery [13]: when high accuracy and target's immobility is desirable (e.g., presence of surgical tools in contact with brain tissue), the stiffness can be tuned as high as possible; vice versa, the device stiffness could be reduced (through the use of a system of active dampers) to allow for limited patient movements and to prevent possible skull damages due to skull clamp pins. The identification of surgical steps allows setting desired working modalities for the newly conceived head restraint. Force/moment values, maximum displacement and frequency content all depends on the surgical workflow step, therefore the behavior of the systems used in the operating room (e.g., the control of a surgical robot) can depend on the particular current step, which could be automatically identified.

These new active head restraint devices should be able to damp the amount of forces and moments reported in this work. On the basis of the performed analysis, the active damper should be able to sustain these maximum values: 70–100 N as exerted external force, 5 mm as displacement,

250 mm/s as velocity and 4.7 m/s<sup>2</sup> as acceleration, with a frequency content of 3 Hz. In addition, the control loop of a surgical robotic assistant can be designed to robustly track and compensate such head motions.

The analysis performed can be also used as a reference for further investigation on patient risks related to restraining head fixation devices. During the whole procedure, the awake patient can progressively slip or shift on the surgical table since he/she is not sedated; a safety system that warns the surgeon when a force threshold is exceeded will prevent fractures (e.g., intracranial hematoma or depressed skull fractures in pediatric patients) [9, 10, 20] and any other adverse effects.

In addition, the collected data are required for designing the control system for the two lightweight arms (KUKA Laboratories, Augsburg, Germany), carrying the neurosurgical tools, which will actively compensate for the patient movements (predictable or not) [7].

**Acknowledgments** This work was supported by the EU Project Grant ACTIVE FP7-ICT-2009-6-270460. Authors would like to thank Elisa Beretta for her precious help during the experimental setup preparation.

## References

- Chao L, Chen K (1997) Shape optimal design and force sensitivity evaluation of six-axis force sensors. *Sens Actuators A* 63:105–112
- D'Amico M, Ferrigno G (1990) Technique for the evaluation of derivatives from noisy biomechanical displacement data using a model-based bandwidth-selection procedure. *Med Biol Eng Comput* 28:407–415
- De Lorenzo D, De Momi E, Dyagilev I, Manganelli R, Formaglio A, Prattichizzo D, Shoham M, Ferrigno G (2011) Force feedback in a piezoelectric linear actuator for neurosurgery. *Int J Med Robot Comput Assisted Surg* 7:268–275
- Donaldson N, Munih M, Perkins T, Wood D (1999) Apparatus to measure simultaneously 14 isometric leg joint moments. Part 1: design and calibration of six-axis transducers for the forces and moments at the ankle. *Med Biol Eng Comput* 37:137–147
- Dreier JD, Williams B, Mangar D, Camporesi EM (2009) Patients selection in awake neurosurgery. *HSR Proc Intensive Care Cardiovasc Anesth* 30:19–27
- Duffau H (2005) Lessons from brain mapping in surgery for low-grade glioma: insights into associations between tumour and brain plasticity. *Lancet Neurol* 4:476–486
- Ferrigno G, Baroni G, Casolo F, De Momi E, Gini G, Matteucci M, Pedrocchi A (2011) Medical robotics. *Pulse IEEE* 2:55–61
- Hemm S, Werdell K (2010) Stereotactic implantation of deep brain stimulation electrodes: a review of technical systems, methods and emerging tools. *Med Biol Eng Comput* 48:611–624
- Lee M, Rezai AR, Chou J (1994) Depressed skull fractures in children secondary to skull clamp fixation devices. *Pediatr Neurosurg* 21:174–7; discussion 178
- Lee MJ, Lin EL (2010) The use of the three-pronged Mayfield head clamp resulting in an intracranial epidural hematoma in an adult patient. *Eur Spine J* 19(Suppl 2):S187–S189
- Liker MA, Won DS, Rao VY, Hua SE (2008) Deep brain stimulation: an evolving technology. *Proc IEEE* 96:1129–1141
- Liu SA, Tzo HL (2002) A novel six-component force sensor of good measurement isotropy and sensitivities. *Sens Actuators A* 100:223–230
- Malosio, M, Negri SP, Pedrocchi N, Vicentini F, Cardinale F, Tosatti LM (2012) The kinematic architecture of the active headframe: a new head support for awake brain surgery. In: Proceedings of the 34th annual international conference of the engineering in medicine and biology society, San Diego, USA
- Mandir AS, Rowland LH, Dougherty PM, Lenz FA (1997) Microelectrode recording and stimulation techniques during stereotactic procedures in the thalamus and pallidum. *Adv Neurol* 74:159–165
- Olivier PE, Du Toit DE (2008) Isokinetic neck strength profile of senior elite rugby union players. *J Sci Med Sport* 11:96–105
- Puangmali P, Althoefer K, Seneviratne LD, Murphy D, Dasgupta P (2008) State-of-the-art in force and tactile sensing for minimally invasive surgery. *Sens J IEEE* 8:371–381
- Rezasoltani A, Ylinen J, Bakhtiary AH, Norozi M, Montazeri M (2008) Cervical muscle strength measurement is dependent on the location of thoracic support. *Br J Sports Med* 42:379–382
- Rozet I, Vavilala MS (2007) Risks and benefits of patient positioning during neurosurgical care. *Anesthesiol Clin* 25:631–653
- Seng KY, Lee Peter VS, Lam PM (2002) Neck muscle strength across the sagittal and coronal planes: an isometric study. *Clin Biomech (Bristol, Avon)* 17:545–547
- Serramito-Garcia R, Arcos-Algaba A, Santin-Amo JM, Garcia-Allut A, Bandin-Dieguez FJ, Gelabert-Gonzalez M (2009) Epidural haematoma due to an headrest in an adult. *Neurocirugia (Astur)* 20:567–570
- Szelenyi A, Bello L, Duffau H, Fava E, Feigl GC, Galanda M, Neuloh G, Signorelli F, Sala F, Workgroup for Intraoperative Management in Low-Grade Glioma Surgery within the European Low-Grade Glioma Network (2010) Intraoperative electrical stimulation in awake craniotomy: methodological aspects of current practice. *Neurosurg Focus* 28:E7
- Trejos AL, Patel RV, Naish MD (2010) Force sensing and its application in minimally invasive surgery and therapy: a survey. *Proc Inst Mech Eng Part C J Mech Eng Sci* 224:1435–1454
- Vasavada AN, Li S, Delp SL (2001) Three-dimensional isometric strength of neck muscles in humans. *Spine (Phila Pa 1976)* 26:1904–1909
- Wang Z, Peng C, Zheng X, Wang P, Wang G (1997) Force measurement on fracture site with external fixation. *Med Biol Eng Comput* 35:289–290